SPE 77539

Three-Phase Displacement Theory: An Improved Description of Relative Permeabilities

Ruben Juanes, SPE, U. C. Berkeley; and **Tad W. Patzek**, SPE, U. C. Berkeley / Lawrence Berkeley National Laboratory

This paper was prepared for presentation at the SPE Annual Technical Conference and Exhibition held in San Antonio, Texas, 29 September–2 October 2002.

Abstract

A quantitative understanding of three-phase flow in porous media is required to address many diverse processes in the subsurface, *e.g.*, improved oil recovery, CO_2 sequestration, and aquifer clean-up. In turn, all predictive models of three-phase flow originate from interpretations of one-dimensional laboratory experiments; when these interpretations are flawed, so are the models. In this paper we revisit the foundations of displacement theory in three-phase flow and provide the most general conditions for *any* relative permeability model to be physical *anywhere* in the saturation triangle. In doing so, we put to rest a controversy that has persisted in petroleum literature for the better part of the last six decades.

When capillarity is ignored, the system of conservation laws describing incompressible immiscible flow should be strictly hyperbolic. This natural property of the system fails for most relative permeability models used today. We identify necessary conditions that relative permeabilities must obey to preserve strict hyperbolicity. These conditions are in agreement with experimental observations and pore-scale physics.

We also present the *most general* analytical solution to the Riemann problem (constant initial and injected states) for three-phase flow, and describe the characteristic waves that may arise, concluding that *only* 9 combinations of rarefactions, shocks and rarefaction-shocks are possible. Some of these wave combinations have been overlooked by many because of the associated conceptual and mathematical difficulties.

The analytical developments presented here will be useful in the planning and interpretation of three-phase displacement experiments, in the formulation of consistent relative permeability models, and in the implementation of streamtube simulators.

Introduction

Three immiscible fluids, water, oil and gas, may flow in many processes of great practical importance: in primary production below bubble point and with movable water; in waterfloods, man-made and natural; immiscible CO_2 floods; steam floods; in some gas condensate reservoirs; in gravity drainage of gas caps with oil and water; WAG processes; and in contaminant intrusions into the shallow subsurface, just to name a few.

Relative permeabilities to water, oil and gas are perhaps the most important rock-fluid descriptors in reservoir engineering. Nowadays, these permeabilities are routinely backed out from the theories of transient, high-rate displacements of inert and incompressible fluids that flow in short cores subjected to very high pressure gradients. More recently, the time evolution of area-averaged fluid saturations was measured with a CT scanner and, with several assumptions,[1] used to estimate the respective relative permeabilities in gravity drainage. Superior precision of the latter approach allowed the determination of relative permeabilities as low as 10^{-6}.

When the fractional flow approach is used, flow of three immiscible incompressible fluids is described by a pressure equation and a 2×2 system of saturation equations.[2] It was long believed that, in the absence of capillarity, the system of equations would be strictly hyperbolic for any relative permeability functions. This is far from being the case and, in fact, loss of strict hyperbolicity occurs for virtually all relative permeability models used today. In this paper we argue that such a behavior is not physically-based, and show how to overcome this deficiency. To do so, we adopt an opposite viewpoint to that of the existing literature: strict hyperbolicity of the system is assumed, and the implications for the functional form of the relative permeabilities are analyzed.

There is a theory behind each quantitative experiment. Not only does any theory reduce and abstract experience, but it also overreaches it by extra assumptions made for definiteness. Theory, in its turn, predicts the results of some specific experiments. The body of theory furnishes the concepts and formulæ by which experiment can be interpreted as being in accord or discord with it. Experiment, indeed, is a *necessary adjunct* to a physical theory; but it is an adjunct, not the master.[3] In other words, the relative permeability models are only as good as theories behind the displacement experiments from which these models have been obtained. If the theory is flawed, so are the relative permeabilities.

Displacement Theory in Three-Phase Flow

Governing Equations. We outline the mathematical formulation of multiphase flow in porous media under the following assumptions: (1) one-dimensional flow; (2) immiscible flow; (3) incompressible fluids; (4) homogeneous rigid porous medium; (5) multiphase flow extension of Darcy's law; (6) negligible gravitational effects; and (7) negligible capillary pressure effects. A detailed derivation of the governing equations can be found elsewhere.[2,4,5]

Assumption 2 prevents mass transfer between phases and, therefore, one can identify components with phases. The one dimensional mass conservation equation for the α-phase is, in the absence of source terms:

$$\partial_t(m_\alpha) + \partial_x(F_\alpha) = 0, \tag{1}$$

where m_α is the mass density, F_α is the mass flux of the α-phase, and $\partial_t(\cdot)$, $\partial_x(\cdot)$ denote partial derivatives with respect to time and space, respectively. For three-phase flow the system consists of aqueous, vapor and liquid phases, corresponding to water (w), gas (g) and oil (o) components, respectively. The mass density of each phase is the mass per unit bulk volume of porous medium:

$$m_\alpha = \rho_\alpha S_\alpha \phi, \tag{2}$$

where ρ_α is the density of the α-phase, S_α is the saturation, and ϕ is the porosity. Assumptions 3 and 4 make the phase densities and the porosity constant. Using the usual multiphase flow extension of Darcy's law[6] (assumption 5):

$$F_\alpha = -k\frac{k_{r\alpha}}{\mu_\alpha}\rho_\alpha(\partial_x p_\alpha + \rho_\alpha g \partial_x z), \tag{3}$$

where k is the absolute permeability, $k_{r\alpha}$ is the relative permeability, μ_α the dynamic viscosity, and p_α the pressure of the α-phase. Relative permeabilities are assumed to be functions of phase saturations. The gravitational acceleration has absolute value g and points in the negative direction of the z-axis. We define the relative mobility of the α-phase as

$$\lambda_\alpha := \frac{k_{r\alpha}}{\mu_\alpha}. \tag{4}$$

Neglecting gravitational and capillarity effects (assumptions 6 and 7) the mass conservation equations for the α-phase is:

$$\partial_t S_\alpha + \partial_x(-\frac{1}{\phi}k\lambda_\alpha \partial_x p) = 0, \tag{5}$$

where p is the pressure, now common to all phases. Since the fluids fill up the pore volume, their saturations add up to one:

$$\sum_{\alpha=1}^{n} S_\alpha \equiv 1. \tag{6}$$

Adding the conservation equations for all phases and using the saturation constraint (6), we get the "pressure equation":

$$\partial_x(-\frac{1}{\phi}k\lambda_T \partial_x p) = 0, \tag{7}$$

where $\lambda_T = \sum_{\alpha=1}^{n}\lambda_\alpha$ is the total mobility. The pressure equation (7) dictates that the total velocity, defined as

$$v_T := -\frac{1}{\phi}k\lambda_T \partial_x p, \tag{8}$$

is at most a function of time. We now define the phase velocity

$$v_\alpha := \frac{\lambda_\alpha}{\lambda_T} v_T, \tag{9}$$

and the fractional flow for the α-phase

$$f_\alpha := \frac{v_\alpha}{v_T} = \frac{\lambda_\alpha}{\lambda_T}. \tag{10}$$

With the definitions above, the *three-phase flow* system is governed by a 2×2 system of conservation laws,

$$\partial_t \begin{pmatrix} S_w \\ S_g \end{pmatrix} + v_T \partial_x \begin{pmatrix} f_w \\ f_g \end{pmatrix} = \begin{pmatrix} 0 \\ 0 \end{pmatrix}, \tag{11}$$

and the algebraic constraint $S_o = 1 - S_w - S_g$. The solution is restricted to lie in the *saturation triangle*:

$$\mathcal{T} := \{(S_w, S_g) : S_w \geq 0, \quad S_g \geq 0, \quad S_w + S_g \leq 1\}. \tag{12}$$

The saturation triangle is usually represented as a ternary diagram (**Fig. 1**), in which the pair (S_w, S_g) corresponds to the triple (S_w, S_g, S_o), where $S_o \equiv 1 - S_w - S_g$.

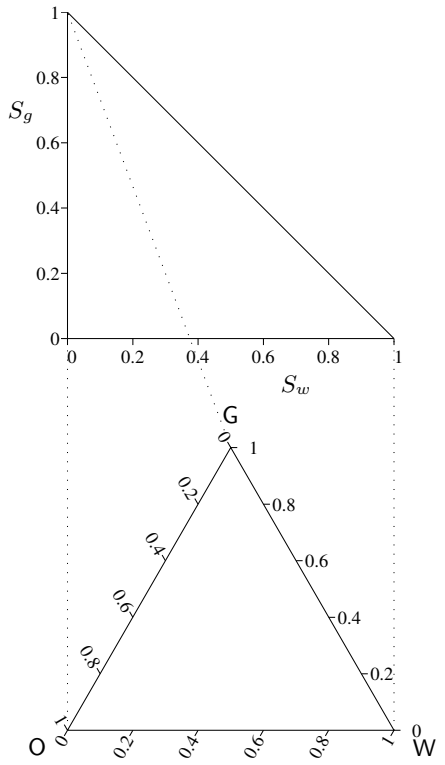

Fig. 1— Saturation triangle (top) and ternary diagram (bottom).

Riemann Problem. Eq. (11) can be written in vector notation defining the vector of unknowns $\boldsymbol{u} = [u, v]^t = [S_w, S_g]^t$, and the flux vector $\boldsymbol{f} = [f, g]^t = [f_w, f_g]^t$. The Riemann problem for three-phase flow consists in finding a self-similar (usually weak) solution to the 2×2 system:

$$\partial_t \boldsymbol{u} + v_T \partial_x \boldsymbol{f} = \boldsymbol{0}, \quad -\infty < x < \infty,\ t > 0, \tag{13}$$

with initial condition

$$\boldsymbol{u}(x, 0) = \begin{cases} \boldsymbol{u}_l & \text{if } x < 0, \\ \boldsymbol{u}_r & \text{if } x > 0. \end{cases} \tag{14}$$

Unrealistic as it may seem (unbounded domain, and piecewise constant initial data with a single discontinuity), the solution to the Riemann problem is extremely valuable for practical applications. Many laboratory experiments reproduce in fact the conditions of the Riemann problem: the medium has initially homogeneous saturations, and the proportion of injected fluids is held constant during the experiment. The solution to the Riemann problem gives also information about the structure of the system of equations, and can be used as the building block for problems with more complex initial conditions (as in the Godunov method[7,8]).

The property of *self-similarity* has been termed "stretching principle"[9] or "coherence condition"[10,11] in the petroleum engineering literature. It means that the solution at different times "can be obtained from one another by a similarity transformation."[12] We seek a solution of the form

$$\boldsymbol{u}(x, t) = \boldsymbol{U}(\zeta). \tag{15}$$

In our case, the similarity variable ζ is

$$\zeta := \frac{x}{\int_0^t v_T(\tau)\, \mathrm{d}\tau} \tag{16}$$

Using Eqs. (15)–(16) in Eq. (13), the self-similar solution satisfies the system of ordinary differential equations

$$(\boldsymbol{A}(\boldsymbol{U}) - \zeta \boldsymbol{I})\boldsymbol{U}' = \boldsymbol{0}, \quad -\infty < \zeta < \infty, \tag{17}$$

together with the boundary conditions

$$\boldsymbol{U}(-\infty) = \boldsymbol{u}_l, \quad \boldsymbol{U}(\infty) = \boldsymbol{u}_r, \tag{18}$$

where $\boldsymbol{A}(\boldsymbol{U})$ is the Jacobian matrix of the system, *i.e.*,

$$\boldsymbol{A}(\boldsymbol{U}) := \mathrm{D}_{\boldsymbol{U}} \boldsymbol{f} = \begin{pmatrix} f_{,u}(\boldsymbol{U}) & f_{,v}(\boldsymbol{U}) \\ g_{,u}(\boldsymbol{U}) & g_{,v}(\boldsymbol{U}) \end{pmatrix}, \tag{19}$$

and $\boldsymbol{I}$ is the 2×2 identity matrix. Subscripts after a comma in Eq. (19) denote differentiation (*e.g.*, $f_{,u} \equiv \partial_u f$).

Character of the System of Equations. Eqs. (17)–(18) define in fact an eigenvalue problem, where ζ is an eigenvalue, and $\boldsymbol{U}' = \mathrm{d}\boldsymbol{U}/\mathrm{d}\zeta$ is a right eigenvector. There are two families of eigenvalues (which we denote ν_1 and ν_2) and eigenvectors ($\boldsymbol{r}_1$ and $\boldsymbol{r}_2$). The eigenvalues and eigenvectors determine the character of the system.

The system is called *hyperbolic* if, for each state $\boldsymbol{U} = (u, v)$, both eigenvalues $\nu_1(\boldsymbol{U})$ and $\nu_2(\boldsymbol{U})$ are real, and the Jacobian matrix $\boldsymbol{A}(\boldsymbol{U})$ is diagonalizable. If, in addition, the eigenvalues are distinct, $\nu_1(\boldsymbol{U}) < \nu_2(\boldsymbol{U})$, the system is called *strictly hyperbolic*. If there is a double eigenvalue and the Jacobian matrix is not diagonalizable, the system is *parabolic*. Finally, if the eigenvalues are complex conjugates at some point $\boldsymbol{U}$, the system is *elliptic* at that point.

The eigenvalues are given by

$$\nu_{1,2} = \frac{1}{2}\left[f_{,u} + g_{,v} \mp \sqrt{(f_{,u} - g_{,v})^2 + 4 f_{,v} g_{,u}} \right]. \tag{20}$$

The eigenvalues are real whenever the discriminant is nonnegative, *i.e.*,

$$\delta := (f_{,u} - g_{,v})^2 + 4 f_{,v} g_{,u} \geq 0, \tag{21}$$

and distinct if the inequality above is strict.

The eigenvectors $\boldsymbol{r}_p = [r_{pu}, r_{pv}]^t$, $p = 1, 2$, of the system are given by the following expressions:

$$\frac{r_{1v}}{r_{1u}} = \frac{\nu_1 - f_{,u}}{f_{,v}} = \frac{g_{,u}}{\nu_1 - g_{,v}}, \tag{22}$$

$$\frac{r_{2u}}{r_{2v}} = \frac{f_{,v}}{\nu_2 - f_{,u}} = \frac{\nu_2 - g_{,v}}{g_{,u}}. \tag{23}$$

The eigenvectors should be normalized so that $|\boldsymbol{r}_p| \equiv 1$.

Relative Permeabilities for Strict Hyperbolicity

Introduction. We assume that pressure and temperature do not greatly influence fluid viscosities, and we take them as constants. Under this assumption, the character of the system is *completely determined* by the relative permeabilities.

Experimental evidence[13–16] suggests that there is a threshold saturation for each phase, below which that phase is immobile. As a result, three-phase flow takes place only in a region inside the saturation triangle. The nature of these threshold saturations depends on the wettability of the fluid, and on the displacement process.[17] For the wetting phase, the term "connate" (or "irreducible") saturation would be appropriate both in drainage and imbibition. For the nonwetting phase, the term "critical" saturation would be applicable in drainage, and "trapped" (or "residual") saturation in imbibition. For the purpose of this paper we lump the terminology above in the term "immobile" saturation $S_{\alpha i}$, regardless of the process. If these endpoint saturations are taken as constants, one can define *reduced saturations* $\tilde{S}_\alpha$ as:

$$\tilde{S}_\alpha := \frac{S_\alpha - S_{\alpha i}}{1 - \sum_{\beta=1}^{3} S_{\beta i}}, \quad \alpha = 1, \ldots, 3. \tag{24}$$

Eqs. (24) define a linear map from the three-phase flow subtriangle (the shaded region in **Fig. 2**) to the whole ternary diagram. It is important to note that the three-phase flow region is not necessarily an equilateral triangle, as the "immobile" saturation of each phase may vary with the saturations of the other two phases. This is a well-known behavior for the oil phase,[18] and several correlations for the "residual" oil saturation have been proposed.[19,20] In this case, the mapping of the three-phase flow region onto the unit ternary diagram would be more complicated than just the linear relation in Eqs. (24).

The relative permeability of a phase is zero if that phase is immobile, and it is positive otherwise. By expressing relative permeabilities as functions of reduced saturations, and using the linear transformation (24), the original system (13) can be written as:

$$\partial_t \tilde{\boldsymbol{u}} + \tilde{v}_T \partial_x \tilde{\boldsymbol{f}}(\tilde{\boldsymbol{u}}) = \boldsymbol{0}, \tag{25}$$

where $\tilde{\boldsymbol{f}}$ is the fractional flow vector expressed as a function of reduced saturations, and

$$\tilde{v}_T = \frac{v_T}{1 - \sum_{\beta=1}^{3} S_{\beta i}} \tag{26}$$

is the reduced total velocity. To simplify notation we shall drop the tildes from Eq. (25), but still refer to the system in terms of reduced saturations.

Loss of Strict Hyperbolicity in Conventional Models. It was long believed that the system (13) was strictly hyperbolic for any relative permeability functions. Then, the theory of Lax[21] as extended by Liu[22,23] would apply.

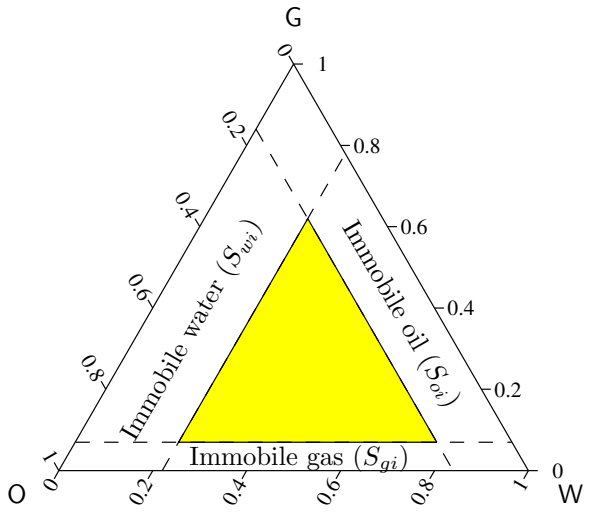

Fig. 2— Schematic of constant immobile saturations for each phase. The three-phase flow region (shaded area) is, in this case, an equilateral triangle inside the ternary diagram.

However, Bell *et al.*[24] showed that the system is not necessarily hyperbolic. In particular, they observed that Stone I relative permeabilities gave rise to *elliptic regions* inside the saturation triangle. Elliptic regions are portions of the saturation triangle where the eigenvalues are complex, so the system is locally elliptic rather than hyperbolic. This implies that boundary conditions need to be imposed at later times to control the solution at earlier times.[20] The analysis of Bell *et al.*[24] shows that the solution is unstable in these regions. One of the consequences is that for arbitrarily close left and right states inside the elliptic region, the solution develops wildly oscillatory waves, which are never observed in experiments. Moreover, the wave pattern is unstable with respect to the initial states.

It was shown[20,25–29] that occurrence of elliptic regions is the rule rather than the exception, for the most common relative permeability models. The analysis of Shearer[25] and Holden[28] starts by assuming the behavior of relative permeabilities at the edges of the saturation triangle. In particular, it is assumed that both the relative permeability of a phase, and its derivative along the normal to the edge of zero reduced saturation of that phase, are identically zero. In addition, certain "interaction conditions" are imposed. These conditions ensure that the right eigenvector that is parallel to the edge is the one associated with the fast characteristic speed, $\boldsymbol{r}_2$.

The *assumed* behavior at the edges has a profound impact on the character of the system. The first consequence is that each vertex of the saturation triangle is an *umbilic point*, *i.e.*, eigenvalues are equal and the system is not strictly hyperbolic at those points. The second one is that an elliptic region must exist inside the saturation triangle. This general result can be proved using ideas of projective geometry.[25,30]

The only models which do not produce elliptic regions

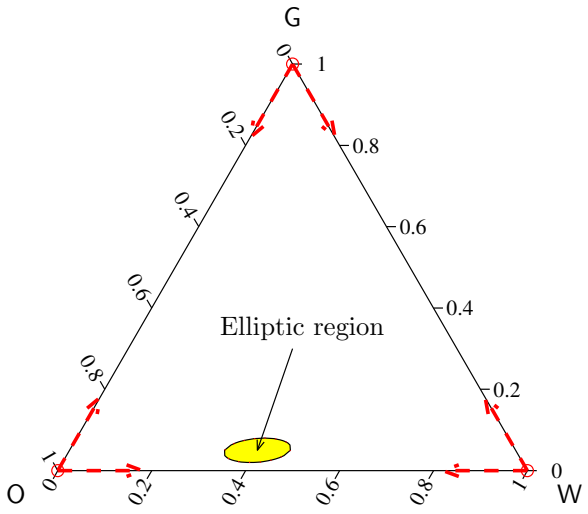

Fig. 3— Schematic representation of the direction of fast eigenvectors r_2 along the edges of the saturation triangle for the models analyzed by Shearer[25,26] and Holden.[28] For models of this type, vertices are umbilic points, and there must be an elliptic region inside the saturation triangle, usually very close to the oil-water edge.

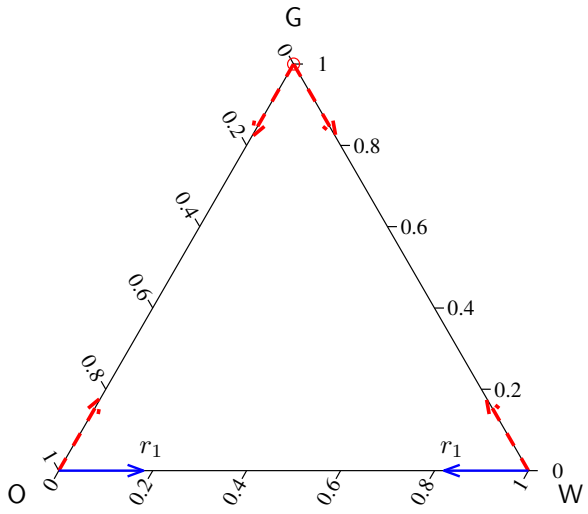

Fig. 4— Schematic representation of the direction of fast (r_2) and slow (r_1) eigenvectors along the edges of the saturation triangle for the type of models we propose. The systems is strictly hyperbolic everywhere inside the saturation triangle, and the only umbilic point is located at the G vertex, where the fast paths corresponding to the OG and WG edges coalesce.

(under the assumed behavior at the edges) are those where the relative permeability of a phase depends solely on the saturation of that phase.[31,32] For these models, the elliptic region shrinks to an isolated umbilic point, which cannot be removed by further approximation of the relative permeabilities. Umbilic points act as "repellers" for classical waves[33,34] and, as a result, solutions to the nonstrictly hyperbolic system require nonclassical waves (termed transitional waves[35]). The most salient features of these solutions are that: (1) they are sensitive to the particular form of the diffusion term due to capillary effects;[36] (2) the saturation path may be the same for wildly different initial and injected states;[33,37,38] and (3) in WAG displacement, the intermediate oil bank may be split in two.[34] Moreover, the Marchesin model (relative permeabilities dependent on their own saturations only) is not supported by experimental results[39] and pore-scale physics.[40]

From the observations above, it is difficult to justify the physical relevance of mathematical singularities like elliptic regions and umbilic points.[2,20,26,32,41–43] We are of the opinion that these singularities are mere artifacts of an *incorrect* mathematical model. Inappropriateness of the formulation may have several sources, the most obvious one being the relative permeability functions and, in particular, the assumed behavior at the edges of the saturation triangle. In fact, it is widely recognized that the slope of experimental relative permeabilities near the endpoints is often ill-defined.[20]

Description of the New Approach. The generic approach in the existing literature can be summarized as follows: a certain behavior of the relative permeabilities is *assumed*, and loss of strict hyperbolicity inside the saturation triangle is *inferred*. We adopt the opposite viewpoint: we assume that the system is strictly hyperbolic, and investigate the conditions on relative permeabilities as functions of saturation such that strict hyperbolicity is preserved.

The *key observation* is that, whenever gas is present as a continuous phase, the mobility of gas is much higher than that of the other two fluids (water and oil). To honor this physical behavior, we associate fast characteristic paths with displacements involving changes in gas saturation, even in the region of small gas saturation. The immediate consequence is that the eigenvector associated with the fast family of characteristics ($\boldsymbol{r}_2$) is *transversal*—and not parallel— to the oil-water edge of the ternary diagram (**Fig. 4**). As we shall see, this conceptual picture permits that the system will be strictly hyperbolic everywhere inside the saturation triangle. The G vertex, corresponding to 100% reduced gas saturation, remains an umbilic point because fast paths corresponding to the OG and WG edges coalesce. This umbilic point could be further removed if one allows for fast eigenvectors to rotate along the OG and WG edges. This was not done here to prevent saturation paths from falling outside the three-phase flow region, but it would be perfectly realistic if, for example, hysteretic effects were considered.

Conditions for Strict Hyperbolicity. Let us recapitulate the conceptual picture expressed in **Fig. 4**:

1. Along the oil-water (OW) edge the eigenvector associated with the *slow* characteristic family ($\boldsymbol{r}_1$) is parallel to the edge. The system is strictly hyperbolic everywhere along the edge, including the O and W vertices.

2. Along the oil-gas (OG) and water-gas (WG) edges the eigenvector associated with the *fast* characteristic family ($\boldsymbol{r}_2$) is parallel to these edges. The system is strictly hyperbolic everywhere along the edges except at the G vertex, which is an umbilic point.

Below we present a *systematic* study of the general conditions that ensure strict hyperbolicity of the system. On each edge we identify two types of conditions. *Condition I* enforces that eigenvectors of the appropriate family are parallel to the edge. *Condition II* guarantees strict hyperbolicity of the system along the edge. The latter condition is further specialized to both vertices of each edge, which provides additional insight into the behavior of the relative permeabilities. The analytical developments are expressed most effectively in terms of water and gas fractional flows (f and g, respectively) and their derivatives with respect to water and gas saturations (u and v, respectively). We then translate these requirements into conditions that the relative permeabilities must satisfy. We emphasize that relative permeabilities and, therefore, relative mobilities, are assumed to be functions of saturations only, *i.e.*,

$$\lambda_w = \lambda_w(u,v),\ \lambda_g = \lambda_g(u,v),\ \lambda_o = \lambda_o(u,v). \tag{27}$$

Due to space restrictions, we present only the main results and their practical implications. The complete analysis is included in a separate publication.[44]

Analysis along the* OW *edge. This edge corresponds to the line of zero reduced gas saturation, $v = 0$. The mathematical condition for the slow eigenvector to be parallel to the OW edge ($\boldsymbol{r}_1 = [1,0]^t$) is:

$$g_{,u} = 0. \tag{28}$$

When expressed in terms of mobilities, Condition I above reads:

$$\lambda_{g,u} = 0, \tag{29}$$

that is, the derivative of the gas relative mobility with respect to water saturation is zero. This condition is immediately satisfied for any model, as the gas mobility is identically zero along this edge.

For the system to be strictly hyperbolic along the OW edge, the following is required:

$$H_{ow} := g_{,v} - f_{,u} > 0, \tag{30}$$

which is equivalent to:

$$\lambda_{g,v} > \lambda_{w,u} - \lambda_{T,u}\frac{\lambda_w}{\lambda_T}. \tag{31}$$

Condition II above is the fundamental requirement for strict hyperbolicity of the system of equations of three-phase flow. When this condition is evaluated at the vertices of the OW edge, one obtains:

$$\lambda_{g,v} > \lambda_{w,u} \quad \text{at the O vertex,} \tag{32}$$
$$\lambda_{g,v} > -\lambda_{o,u} \quad \text{at the W vertex,} \tag{33}$$

where the inequalities above are strict. In particular, Eqs. (32)–(33) require that the gas relative permeability does *not* have zero-derivative at its endpoint saturation. A summary of the conditions at the OW edge is given in **Table 1**. We make the following important remarks:

1. The requirement of a nonzero endpoint slope of the gas relative permeability is a *necessary* condition for strict hyperbolicity, which is violated by the models of all previous studies on this subject.

2. This behavior of gas relative permeability is in good agreement with experimental observations of two-phase[13–15,17,45,46] and three-phase flow,[16,39,47–50] both in drainage and imbibition.

3. A finite positive slope for the gas relative permeability can also be justified from the point of view of pore-scale processes.[51,52] Gas is always the nonwetting fluid, so gas flow takes place through the middle region of the pores (bulk flow). In a drainage process, gas flow will start with the *first percolating* cluster. Likewise, in an imbibition process, gas flow will cease with the *last trapped* cluster. In both cases, the transition between zero flow and nonzero flow is rather abrupt, thus justifying the existence of a positive slope at the endpoint of the relative permeability curve.

4. In contrast, near their endpoint saturations, the most wetting and intermediate wetting fluids flow through a continuous network of films (corner flow and/or film flow). The effective cross-sectional area of this network will vary depending on the local level of capillary pressure. Since the fluid conductance is proportional to the cross-sectional area, it seems plausible that that the relative permeability will approach zero as a quadratic function of saturation and, thus, with zero slope.

Analysis along the* OG *edge. This edge corresponds to the line of zero reduced water saturation, $u = 0$. The fast eigenvector will be parallel to the OG edge ($\boldsymbol{r}_2 = [0,1]^t$) if:

$$f_{,v} = 0. \tag{34}$$

In terms of mobilities, Condition I reads:

$$\lambda_{w,v} = 0, \tag{35}$$

Table 1— Summary of conditions along the OW edge

Condition	Frac. flows		Mobilities
I	$g_{,u} = 0$	$\Leftrightarrow$	$\lambda_{g,u} = 0$
II	$g_{,v} - f_{,u} > 0$	$\Leftrightarrow$	$\lambda_{g,v} > \lambda_{w,u} - \lambda_{T,u}\frac{\lambda_w}{\lambda_T}$
II at O			$\lambda_{g,v} > \lambda_{w,u}$
II at W			$\lambda_{g,v} > -\lambda_{o,u}$

that is, the derivative of the water relative mobility with respect to gas saturation is zero. This condition is immediately satisfied because water mobility is identically zero along this edge.

The system is strictly hyperbolic along the OG edge (Condition II) if:

$$H_{og} := g_{,v} - f_{,u} > 0, \tag{36}$$

or, equivalently:

$$\lambda_{g,v} > \lambda_{w,u} + \lambda_{T,v}\frac{\lambda_g}{\lambda_T}. \tag{37}$$

We want the condition above to be a strict inequality at the O vertex:

$$\lambda_{g,v} > \lambda_{w,u}, \tag{38}$$

and an equality at the G vertex (umbilic point):

$$\lambda_{w,u} = 0. \tag{39}$$

Eq. (38) requires again that the gas relative permeability has a positive slope at its endpoint saturation. The conditions at the OG edge are summarized in **Table 2**.

Analysis along the* WG *edge. This edge corresponds to the line of zero reduced oil saturation, $v = 1 - u$. The analysis at the WG edge is complicated by the fact that it is a tilted line in the (u, v)-plane. The fast eigenvector will be parallel to the WG edge ($\boldsymbol{r}_2 = [-1, 1]^t$) if:

$$f_{,v} + g_{,v} = f_{,u} + g_{,u}. \tag{40}$$

In terms of mobilities, Condition I reads:

$$\lambda_{o,v} = \lambda_{o,u}, \tag{41}$$

that is, the derivatives of the oil relative mobility with respect to gas and water saturations are equal.

The system is strictly hyperbolic along the WG edge (Condition II) if:

$$H_{wg} := g_{,v} - f_{,u} - 2g_{,u} > 0, \tag{42}$$

or, equivalently:

$$-\lambda_{g,u} + \lambda_{g,v} > -\lambda_{o,u} + (\lambda_{T,v} - \lambda_{T,u})\frac{\lambda_g}{\lambda_T}. \tag{43}$$

The strict inequality at the W vertex reads:

$$\lambda_{g,v} > -\lambda_{o,u}, \tag{44}$$

and the equality at the G vertex (umbilic point) imposes that

$$\lambda_{o,u} = 0. \tag{45}$$

Table 3 summarizes the conditions at the WG edge.

Table 2— Summary of conditions along the OG edge

Condition	Frac. flows		Mobilities
I	$f_{,v} = 0$	$\Leftrightarrow$	$\lambda_{w,v} = 0$
II	$g_{,v} - f_{,u} > 0$	$\Leftrightarrow$	$\lambda_{g,v} > \lambda_{w,u} + \lambda_{T,v}\frac{\lambda_g}{\lambda_T}$
II at O			$\lambda_{g,v} > \lambda_{w,u}$
II at G			$\lambda_{w,u} = 0$

A Simple Model. Our interest here reduces to presenting a simple model that satisfies the conditions above. A common practice in petroleum engineering[53,54] is to assume that relative permeabilities of the most and least wetting fluids (usually water and gas) depend only on their own saturation, whereas the relative permeability of the intermediate wetting fluid (usually oil) depends on all saturations. Although we do *not* defend this assumption in general, here we show that it is possible to obtain models which are strictly hyperbolic everywhere in the three-phase flow region. We take, for example:

$$\lambda_w = (1/\mu_w)u^2, \tag{46}$$

$$\lambda_g = (1/\mu_g)\left(\beta_g v + (1-\beta_g)v^2\right), \quad \beta_g > 0 \tag{47}$$

$$\lambda_o = (1/\mu_o)(1-u-v)(1-u)(1-v). \tag{48}$$

The most important feature of the model is the positive derivative of the gas relative permeability function as it approaches zero. For the particular function used here, oil isoperms are slightly convex.[44]

It is immediate to check that relative mobilities (46)–(48) satisfy Condition I on all three edges. Whether Condition II is satisfied will depend, in general, on the values of the fluid viscosities and the endpoint-slope of the gas relative permeability. Rather than performing a complete analysis,[44] we simply take reasonable values of the viscosities:

$$\mu_w = 0.875, \quad \mu_g = 0.03, \quad \mu_o = 2, \tag{49}$$

and a small value of the endpoint slope: $\beta_g = 0.1$.

In **Fig. 5** we represent graphically the functions $H_{ow}(u)$ along OW, $H_{og}(v)$ along OG, and $H_{wg}(u)$ along WG. Inequalities (30), (36), and (42) are satisfied (and the system is strictly hyperbolic) if all three curves are positive everywhere. The curves for the OG edge and the WG edge reach a zero value for $v = 1$ and $u = 0$, respectively, so that the G vertex is an umbilic point.

Analytical Solution to the Riemann Problem

Introduction. Here we present the solution to the Riemann problem of three-phase flow, given by Eqs. (13)–(14). As discussed in the previous section, the system is assumed to be strictly hyperbolic for all saturation paths of interest. For a strictly hyperbolic system, waves of different characteristic families are strictly separated.[21] Thus, the solution to the Riemann problem comprises three constant states $\boldsymbol{u}_l, \boldsymbol{u}_m, \boldsymbol{u}_r$ (left, middle, and right states, respectively). States $\boldsymbol{u}_l$ and $\boldsymbol{u}_m$ are joined by a wave of the

Table 3— Summary of conditions along the WG edge

Condition	Frac. flows		Mobilities
I	$f_{,v} + g_{,v} = f_{,u} + g_{,u}$	$\Leftrightarrow$	$\lambda_{o,v} = \lambda_{o,u}$
II	$g_{,v} - f_{,u} - 2g_{,u} > 0$	$\Leftrightarrow$	$\lambda_{g,v} - \lambda_{g,u} > -\lambda_{o,u} + (\lambda_{T,v} - \lambda_{T,u})\frac{\lambda_g}{\lambda_T}$
II at W			$\lambda_{g,v} > -\lambda_{o,u}$
II at G			$\lambda_{o,u} = 0$

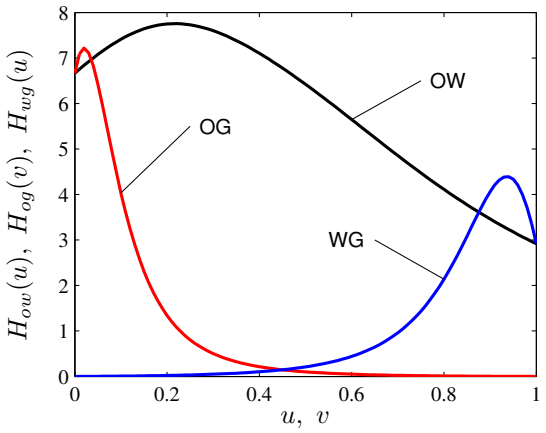

Fig. 5— Strict hyperbolicity on edges of the saturation triangle (Condition II) requires that all three functions $H_{ow}(u)$, $H_{og}(v)$, and $H_{wg}(u)$ are positive everywhere.

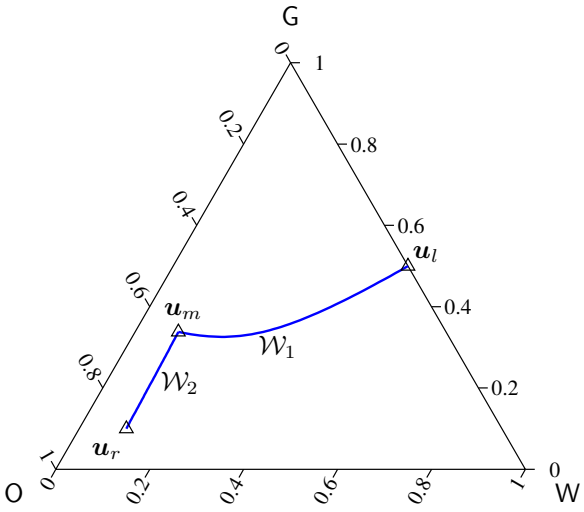

Fig. 6— Generic solution to the Riemann problem of three-phase flow with two waves connecting three constant states.

first family (slow wave, or 1-wave), and states $\boldsymbol{u}_m$ and $\boldsymbol{u}_r$ are joined by a wave of the second family (fast wave, or 2-wave). We conclude that the solution to the Riemann problem for three-phase flow reduces to finding the intermediate constant state $\boldsymbol{u}_m$ as the intersection of an admissible 1-wave ($\mathcal{W}_1$) and an admissible 2-wave ($\mathcal{W}_2$) on the saturation triangle (**Fig. 6**):

$$\boldsymbol{u}_l \xrightarrow{\mathcal{W}_1} \boldsymbol{u}_m \xrightarrow{\mathcal{W}_2} \boldsymbol{u}_r. \tag{50}$$

Wave Structure. We now describe the structure of the waves in the Riemann solution. From the theory of strictly hyperbolic conservation laws,[21,55] a wave of the p-family consists of p-rarefactions, p-shocks and/or p-contact discontinuities. This is discussed next.

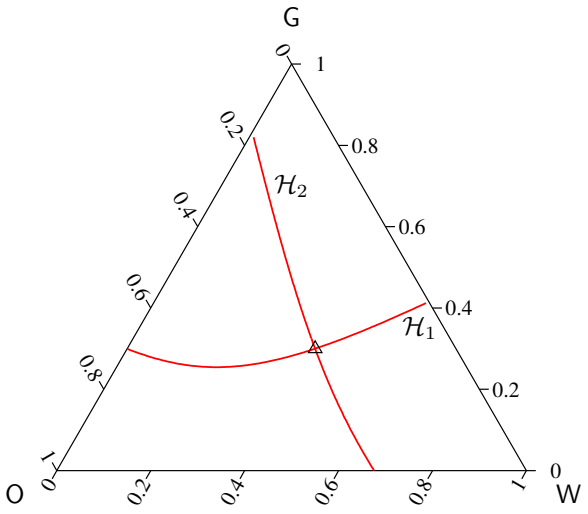

Fig. 7— Typical plot of the Hugoniot loci for both characteristic families passing through the reference state $\triangle$.

Hugoniot loci and shocks. Any propagating discontinuity connecting two states $\boldsymbol{u}_- = \boldsymbol{U}(\zeta_-)$ and $\boldsymbol{u}_+ = \boldsymbol{U}(\zeta_+)$, must satisfy an integral conservation equation for each variable, known as the *Rankine-Hugoniot jump condition*:[8]

$$\boldsymbol{f}(\boldsymbol{u}_+) - \boldsymbol{f}(\boldsymbol{u}_-) = \sigma(\boldsymbol{u}_+;\boldsymbol{u}_-)\big(\boldsymbol{u}_+ - \boldsymbol{u}_-\big), \tag{51}$$

where $\sigma(\boldsymbol{u}_+;\boldsymbol{u}_-)$ is the speed of propagation of the discontinuity. For a fixed state $\boldsymbol{u}_-$, one can determine the set of states $\boldsymbol{u}_+$ which can be connected to $\boldsymbol{u}_-$ such that Eq. (51) is satisfied. There are two families of solutions, one for each characteristic family, which form two curves passing through the reference state $\boldsymbol{u}_-$: $\mathcal{H}_1(\boldsymbol{u}_-)$ and $\mathcal{H}_2(\boldsymbol{u}_-)$ (**Fig. 7**). The set of points on each of these curves is called the *Hugoniot locus*. It is easy to show[8] that the Hugoniot curves are tangent to the corresponding eigenvectors at the reference point $\boldsymbol{u}_-$. Moreover, since the system is strictly hyperbolic, Hugoniot loci do not have detached branches and are transversal to each other.[55]

Not every discontinuity satisfying the Rankine-Hugoniot condition is a valid shock. For a genuine shock of the p-family (a p-shock) to be physically admissible, it must satisfy the *Lax entropy condition*:[8,21,56]

$$\nu_p(\boldsymbol{u}_-) > \sigma_p(\boldsymbol{u}_+;\boldsymbol{u}_-) > \nu_p(\boldsymbol{u}_+), \tag{52}$$

where $\boldsymbol{u}_-$ and $\boldsymbol{u}_+$ are the values at the left and at the right of the discontinuity, respectively. Condition (52) implies that characteristics of the p-family go *into* the shock. A shock curve of the p-family passing through point $\boldsymbol{u}_-$, denoted as $\mathcal{S}_p(\boldsymbol{u}_-)$, corresponds to a subset of the Hugoniot locus $\mathcal{H}_p(\boldsymbol{u}_-)$, for which entropy condition (52) is satisfied.

Integral curves and rarefactions. A curve whose tangent at any point $\boldsymbol{u}$ lies in the direction of the right eigenvector $\boldsymbol{r}_p(\boldsymbol{u})$ is called an *integral curve* for the p-family. There are two integral curves passing through each

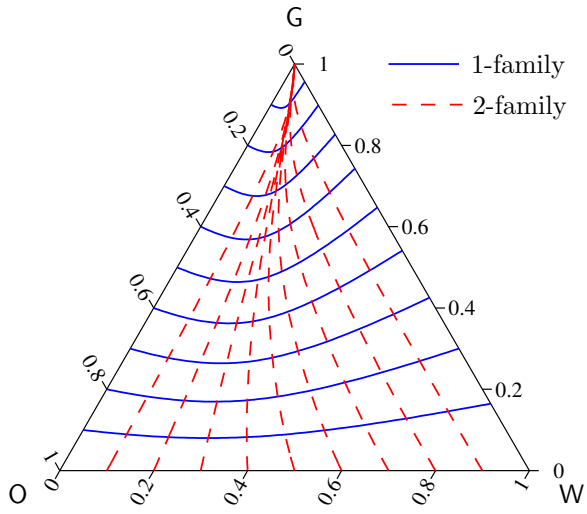

Fig. 8— Typical plot of the integral curves (usually termed slow paths and fast paths) for a relative permeability model that produces a strictly hyperbolic system.

reference point $\hat{\boldsymbol{u}}$: $\mathcal{I}_1(\hat{\boldsymbol{u}})$, corresponding to the first eigenvector $\boldsymbol{r}_1$, and $\mathcal{I}_2(\hat{\boldsymbol{u}})$, corresponding to the second eigenvector $\boldsymbol{r}_2$. The two families of integral curves for the relative permeability model discussed in the previous section (Eqs. (46)–(47)) are shown in **Fig. 8**.

A necessary condition for two states $\boldsymbol{u}_l$ (left) and $\boldsymbol{u}_r$ (right) to be connected by a rarefaction wave is that these two states lie on the same integral curve.[8,21] Therefore, a rarefaction curve of the p-family (hereafter noted $\mathcal{R}_p$), is a subset of integral curve $\mathcal{I}_p$, much in the same way as a shock curve is a subset of the corresponding Hugoniot locus. A p-rarefaction wave is a self-similar solution $\boldsymbol{U}_p(\zeta)$ satisfying Eq. (17) where the parameter ζ is not arbitrary, but an eigenvalue of the problem:[8]

$$\zeta = \nu_p(\boldsymbol{U}_p(\zeta)). \tag{53}$$

A rarefaction curve $\boldsymbol{U}_p(\zeta)$ will provide a single-valued solution if the similarity variable parameter ζ (*i.e.*, the eigenvalue ν_p) increases *monotonically* along the curve from the left state $\boldsymbol{u}_l$ to the right state $\boldsymbol{u}_r$.

Inflection loci and rarefaction-shocks. The notion of genuine nonlinearity is crucial to the wave structure arising in multiphase flow. The p-field is said to be *genuinely nonlinear* if the p-eigenvalue ν_p varies monotonically along integral curves of the p-family. This is expressed mathematically as:

$$\nabla\nu_p(\boldsymbol{U}) \cdot \boldsymbol{r}_p(\boldsymbol{U}) \neq 0 \quad \text{for all } \boldsymbol{U}, \tag{54}$$

where $\nabla\nu_p(\boldsymbol{U}) := [\partial\nu_p/\partial u, \partial\nu_p/\partial v]^t$ is the gradient of $\nu_p(\boldsymbol{U})$. This condition is equivalent to that of convexity, $f''(u) \neq 0\ \forall u$, for scalar conservation laws. The p-field is said to be *linearly degenerate* if ν_p is constant along integral curves of the p-family, *i.e.*,

$$\nabla\nu_p(\boldsymbol{U}) \cdot \boldsymbol{r}_p(\boldsymbol{U}) \equiv 0 \quad \text{for all } \boldsymbol{U}. \tag{55}$$

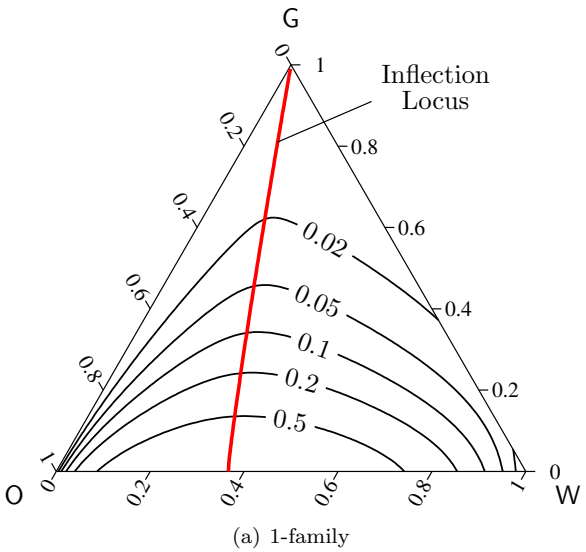

(a) 1-family

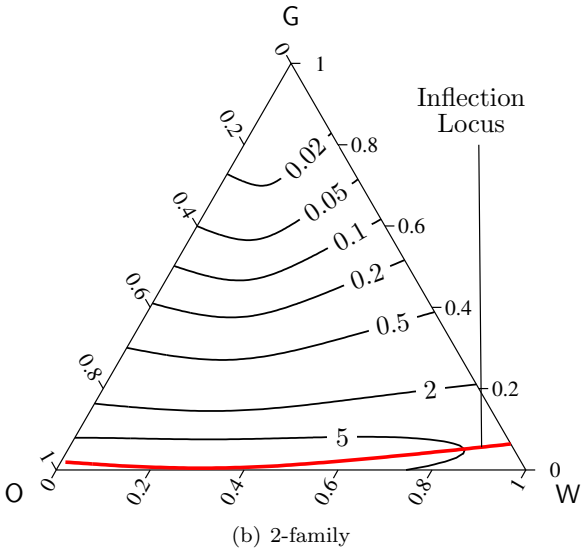

(b) 2-family

Fig. 9— Eigenvalues and inflection loci for both families of characteristics. Inflection loci correspond to local maxima of eigenvalues when moving along integral curves.

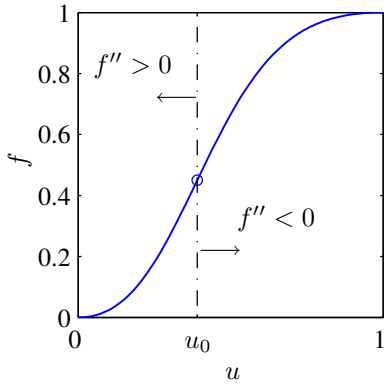

Fig. 10— Typical plot of the flux function f (fractional flow) for two-phase flow. The function is S-shaped, and the slope attains a maximum value at the inflection point u_0.

Of course, the value of $\nu_p(\boldsymbol{U})$ may vary from one integral curve to the next. As it turns out, the characteristic fields of the system describing three-phase flow are neither genuinely nonlinear nor linearly degenerate: eigenvalues attain local maxima along integral curves. We can therefore define the *inflection locus* $\mathcal{V}_p$ for the p-characteristic field as the set of points $\boldsymbol{U}$ such that

$$\nabla\nu_p(\boldsymbol{U}) \cdot \boldsymbol{r}_p(\boldsymbol{U}) = 0, \tag{56}$$

that is, the locations at which ν_p attain either a maximum or a minimum value when moving along integral curves of the p-family. In **Fig. 9** we show contour plots of eigenvalues and the inflection loci for both characteristic families. We note that in *all* realistic models of multiphase flow, the inflection locus corresponds to *maxima* of eigenvalues. This is consistent with the well-known behavior of the flux function for the two-phase flow case, where the fractional flow function is S-shaped, and the inflection point corresponds to the *maximum value* of the derivative (**Fig. 10**).

For a strictly hyperbolic system whose characteristic fields are genuinely nonlinear, any wave connecting two states $\boldsymbol{u}_l$ and $\boldsymbol{u}_r$ can only be a rarefaction or a genuine shock, and any discontinuity must satisfy Lax entropy condition (52). When the genuine nonlinearity condition fails, each wave might consist in a combination of rarefactions and discontinuities.[22,23] For strictly hyperbolic models of multiphase flow, the inflection locus for each field is a single connected curve, which is transversal to integral curves of the same family. In this case, the composite wave has at most one rarefaction and one discontinuity. Moreover, since inflection loci correspond to local *maxima* of eigenvalues along integral curves, the rarefaction is always slower than the shock.[57] It follows that a wave consisting of a shock followed by a rarefaction is *not* possible.

More precisely, a rarefaction-shock of the p-family connecting the left and right states $\boldsymbol{u}_l$ and $\boldsymbol{u}_r$, respectively, is a curve on the phase plane consisting of a p-rarefaction curve emanating from $\boldsymbol{u}_l$, connected to a p-shock curve at some intermediate point $\boldsymbol{u}_*$, which ends at the right state. This rarefaction-shock curve is denoted as $\mathcal{R}_p\mathcal{S}_p(\boldsymbol{u}_r;\boldsymbol{u}_l)$ and, unlike rarefaction curves or shock curves alone, is defined through both endpoints. The intermediate state $\boldsymbol{u}_*$ is the post-shock state, at which the following property holds:

$$\nu_p(\boldsymbol{u}_*) = \sigma_p(\boldsymbol{u}_r;\boldsymbol{u}_*). \tag{57}$$

A necessary condition for a $\mathcal{R}_p\mathcal{S}_p(\boldsymbol{u}_r,\boldsymbol{u}_l)$ wave is that the left and right states lie on opposite sides with respect to the inflection locus $\mathcal{V}_p$. This rules out the possibility of such two states being connected by a rarefaction wave, since the characteristic speed would not be monotonically increasing and, as a result, the solution would not be single-valued. This composite wave also satisfies Liu's extended entropy condition,[22] which reduces to the extended Lax entropy condition[21] (originally developed for systems with genuinely nonlinear and linearly degenerate fields) when the inflection locus is a single hypersurface.[57] Therefore,

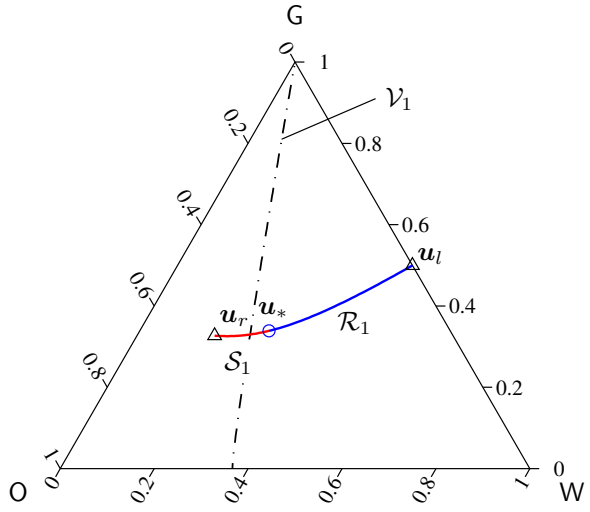

(a) Right state with $u_r \approx 0.17$

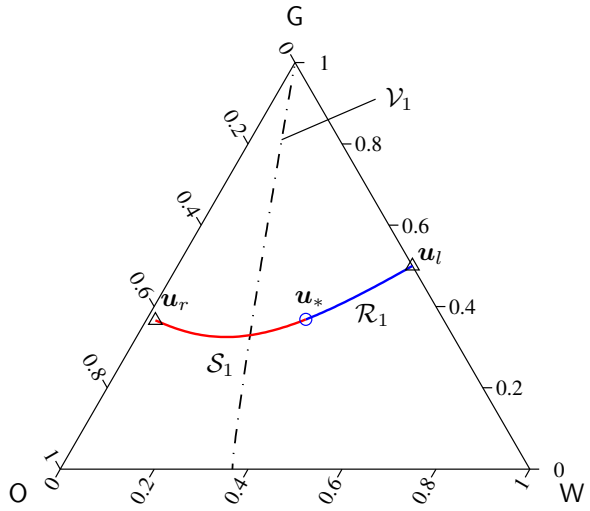

(b) Right state with $u_r \approx 0.02$

Fig. 11— Rarefaction-shock curves for the 1-family with the same left state and two different right states. Note that the post-shock state u_* is different for each case.

all discontinuities must satisfy

$$\nu_p(\boldsymbol{u}_-) \geq \sigma_p(\boldsymbol{u}_+;\boldsymbol{u}_-) > \nu_p(\boldsymbol{u}_+). \tag{58}$$

Fig. 11 shows two rarefaction-shock curves for the first characteristic family, corresponding to the same left state but two different right states. Note that the post-shock state $\boldsymbol{u}_*$, at which the $\mathcal{R}_1$ and $\mathcal{S}_1$ curves are connected, is different for each case. This connection is always very smooth. In fact, it can be shown[21] that both curves are connected with second order tangency (same slope and curvature).

Complete Set of Solutions. Based on the analysis above, a wave of the p-family connecting two constant states may only be one of the following: a p-rarefaction

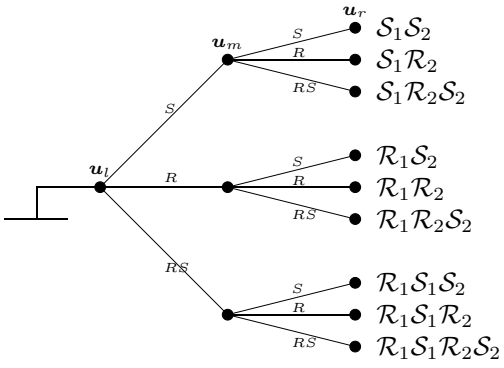

Fig. 12— Schematic tree with all 9 possible combinations of solutions to the Riemann problem of three-phase flow.

($\mathcal{R}_p$), a p-shock ($\mathcal{S}_p$), or a p-rarefaction-shock ($\mathcal{R}_p\mathcal{S}_p$). Since the full solution to the Riemann problem is a sequence of two waves, $\mathcal{W}_1$ and $\mathcal{W}_2$, there are *only 9* possible combinations of solutions. A schematic tree with all possible solution types are shown in **Fig. 12**.

Example:* $\mathcal{R}_1\mathcal{S}_1\mathcal{R}_2\mathcal{S}_2$ *solution. We describe in some detail the case with the most complicated wave structure that may arise in the Riemann problem of three-phase flow. In this case both waves are composite rarefaction-shocks: $\mathcal{W}_1 \equiv \mathcal{R}_1\mathcal{S}_1$ and $\mathcal{W}_2 \equiv \mathcal{R}_2\mathcal{S}_2$.

The variables that need to be determined to fully characterize the solution are: the intermediate constant state $\boldsymbol{u}_m$, the shock speeds σ_1 and σ_2, and the post-shock states $\boldsymbol{u}_1^*$ and $\boldsymbol{u}_2^*$ of each wave. The constant state $\boldsymbol{u}_m$ corresponds to the intersection of the two wave curves, while the post-shock states are the points where the rarefaction curve and the shock curve of the same family are joined. Schematically, this can be represented as follows:

$$\boldsymbol{u}_l \xrightarrow{\mathcal{R}_1} \boldsymbol{u}_1^* \xrightarrow{\mathcal{S}_1} \boldsymbol{u}_m \xrightarrow{\mathcal{R}_2} \boldsymbol{u}_2^* \xrightarrow{\mathcal{S}_2} \boldsymbol{u}_r. \tag{59}$$

The solution is admissible if each of the two waves is admissible individually, *i.e.*,

$$\begin{aligned} \mathcal{R}_1\mathcal{S}_1: &\begin{cases} \nu_1 \text{ increases monotonically along } \boldsymbol{u}_l \xrightarrow{\mathcal{R}_1} \boldsymbol{u}_1^*, \\ \nu_1(\boldsymbol{u}_1^*) = \sigma_1 > \nu_1(\boldsymbol{u}_m), \end{cases} \\ \mathcal{R}_2\mathcal{S}_2: &\begin{cases} \nu_2 \text{ increases monotonically along } \boldsymbol{u}_m \xrightarrow{\mathcal{R}_2} \boldsymbol{u}_2^*, \\ \nu_2(\boldsymbol{u}_2^*) = \sigma_2 > \nu_2(\boldsymbol{u}_r). \end{cases} \end{aligned} \tag{60}$$

The major difficulty in computing the solution is that both endpoints of the $\mathcal{R}_2$ curve are unknown, so that the initial condition for the integral curve is not know *a priori*. We have developed efficient algorithms for the solution of this highly nonlinear problem. They are based on a predictor-corrector strategy combined with Newton's method, and they yield quadratic convergence in all cases.[58]

In **Fig. 13** we represent the solution as a saturation path in the ternary diagram. It is immediate to check that the solution is admissible. Each composite wave crosses the inflection locus of the corresponding family. We note that the 2-shock has a very small amplitude because the right state almost coincides with the inflection locus of the 2-family.

Profiles of wave speeds ν_1 and ν_2, and phase saturations S_w, S_g and S_o, are plotted in **Fig. 14**. These quantities are plotted against the similarity variable ζ, defined in Eq. (16). We decided to split each plot into two and use a different scale on the ζ-axis, due to the very different speeds of the 1- and 2-wave. Otherwise, the structure of the 1-rarefaction-shock would not be visible on the plots. Points $a < b < c < d$ on the ζ-axis correspond to the wave speeds $\nu_1(\boldsymbol{u}_l) < \sigma_1 < \nu_2(\boldsymbol{u}_m) < \sigma_2$.

Remaining types of solution. For completeness, we present in **Fig. 15** the saturation paths in the ternary diagram for *all 9* solution types. These are:

(a) $\mathcal{S}_1\mathcal{S}_2$: both waves are genuine shocks and, therefore, the solution comprises three constant states separated by two discontinuities.

(b) $\mathcal{S}_1\mathcal{R}_2$: the solution consists of a 1-shock and a 2-rarefaction.

(c) $\mathcal{S}_1\mathcal{R}_2\mathcal{S}_2$: the solution comprises a genuine 1-shock through the left state and a composite 2-rarefaction-shock through the right state.

(d) $\mathcal{R}_1\mathcal{S}_2$: the left state and the right state are joined by a 1-rarefaction followed by a 2-shock.

(e) $\mathcal{R}_1\mathcal{R}_2$: both waves are rarefactions, so the solution is continuous everywhere.

(f) $\mathcal{R}_1\mathcal{R}_2\mathcal{S}_2$: a 1-rarefaction from the left state is followed by a composite 2-rarefaction-shock to the right state.

(g) $\mathcal{R}_1\mathcal{S}_1\mathcal{S}_2$: the slow wave emanating from the left state is a composite rarefaction-shock, which is followed by a genuine 2-shock to the right state.

(h) $\mathcal{R}_1\mathcal{S}_1\mathcal{R}_2$: the left state is joined to the intermediate constant state by a composite rarefaction-shock, and the right state is reached along a 2-rarefaction.

(i) $\mathcal{R}_1\mathcal{S}_1\mathcal{R}_2\mathcal{S}_2$: both waves are rarefaction-shocks.

All cases discussed above give a *complete set of solutions* to the Riemann problem of three-phase flow, under the following assumptions: (1) the system is strictly hyperbolic; and (2) inflection loci are single connected curves, transversal to the integral curves, and correspond to maxima of the eigenvalues.

The widely used conceptual model of three-phase flow as consisting of two successive two-phase flow displacements[10,59,60] can now be understood in the context of the complete solution. This model is an approximation to the actual solution, which assumes that each wave ($\mathcal{W}_1$ and $\mathcal{W}_2$) is parallel to one of the edges of the ternary diagram. Of course, this approximation is accurate only under very restrictive initial and injected conditions.

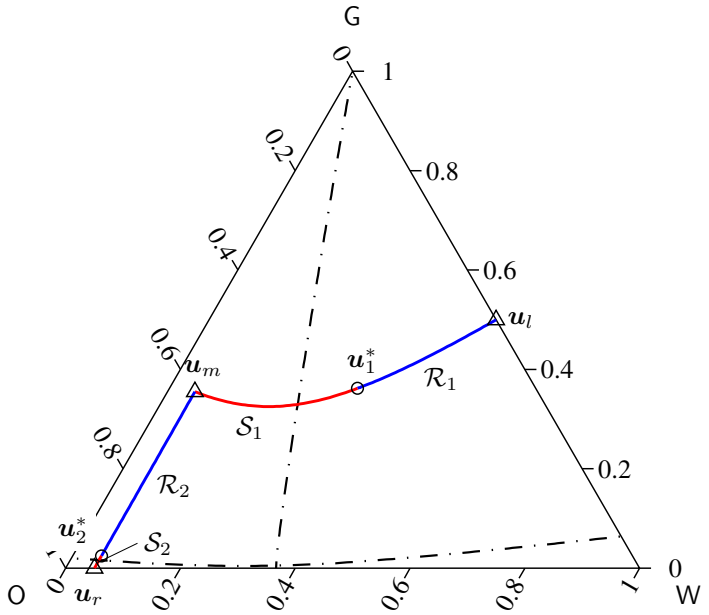

Fig. 13— $\mathcal{R}_1\mathcal{S}_1\mathcal{R}_2\mathcal{S}_2$ solution path in the ternary diagram. Both waves are rarefaction-shocks, which intersect at the intermediate constant state u_m. The post-shock states u_1^* and u_2^* correspond to the points where the rarefaction curve and the shock curve of the same family are joined.

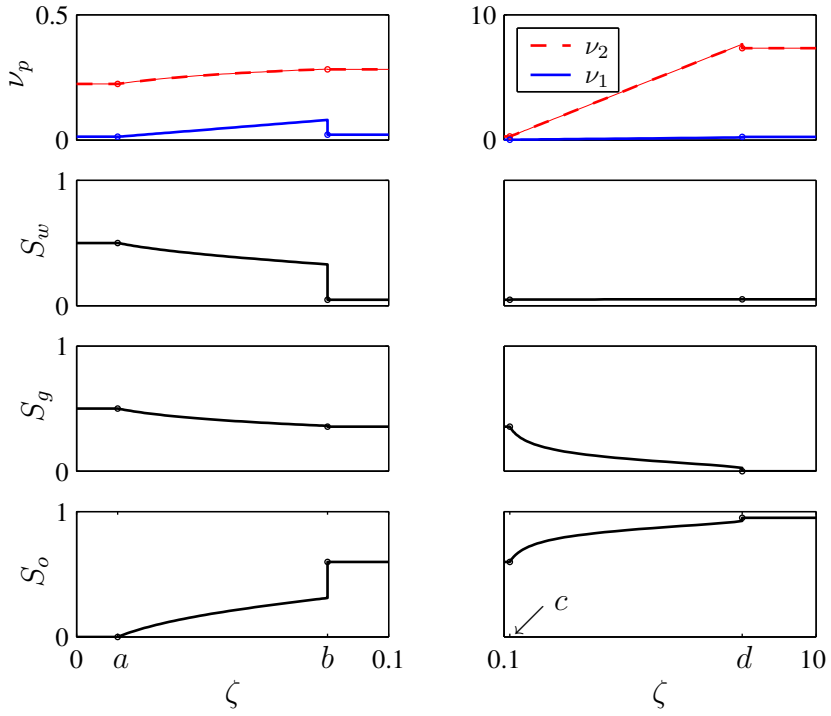

Fig. 14— Profiles of wave speeds ν_1 and ν_2, and phase saturations S_w, S_g and S_o, for the $\mathcal{R}_1\mathcal{S}_1\mathcal{R}_2\mathcal{S}_2$ solution. The solution is plotted against the similarity variable ζ. Points $a < b < c < d$ on the ζ-axis correspond to the wave speeds $\nu_1(u_l) < \sigma_1 < \nu_2(u_m) < \sigma_2$.

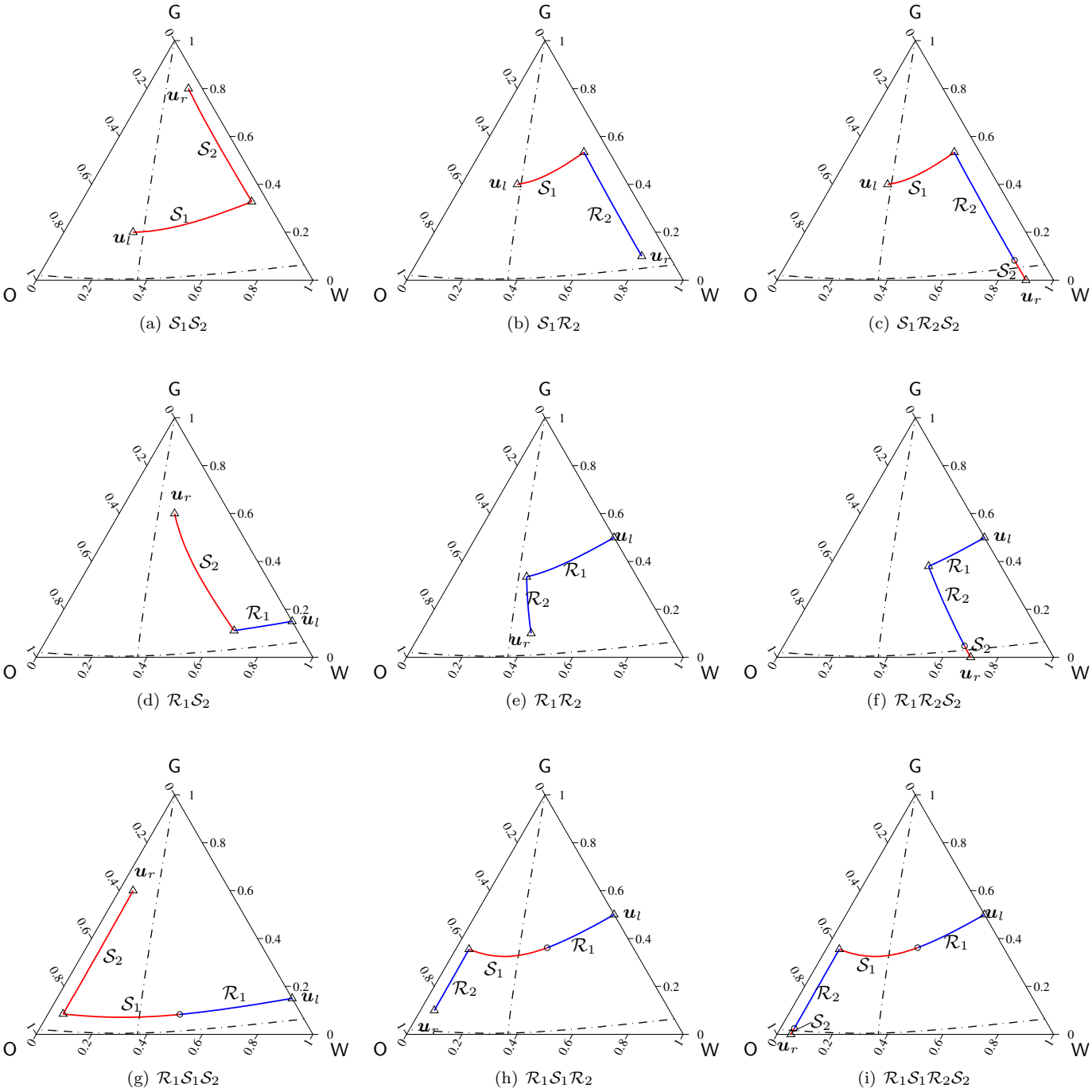

(a) $\mathcal{S}_1\mathcal{S}_2$ (b) $\mathcal{S}_1\mathcal{R}_2$ (c) $\mathcal{S}_1\mathcal{R}_2\mathcal{S}_2$

(d) $\mathcal{R}_1\mathcal{S}_2$ (e) $\mathcal{R}_1\mathcal{R}_2$ (f) $\mathcal{R}_1\mathcal{R}_2\mathcal{S}_2$

(g) $\mathcal{R}_1\mathcal{S}_1\mathcal{S}_2$ (h) $\mathcal{R}_1\mathcal{S}_1\mathcal{R}_2$ (i) $\mathcal{R}_1\mathcal{S}_1\mathcal{R}_2\mathcal{S}_2$

Fig. 15— Examples of saturation paths for all 9 solution types. These 9 cases constitute the complete set of solutions to the Riemann problem of three-phase flow.

Conclusions

Following the unambiguous hints from physics, we have *first* assumed the strict hyperbolicity of the system of equations describing three-phase immiscible flow, and *then* investigated the conditions on relative permeabilities that follow from this assumption. The mathematical derivations presented here lead to meaningful conclusions that agree with experimental observations and pore-scale physics. Our paper has two key results:

1. The derivation of general conditions on relative permeabilities necessary to preserve strict hyperbolicity.

2. The presentation of the *complete* general solution to the Riemann problem of three-phase, incompressible and immiscible flow.

It turns out that a physically reasonable assumption of a finite positive slope of the gas relative permeability function is the most serious condition that must be imposed so that all three relative permeabilities are strictly hyperbolic everywhere in the three-phase flow region. For a commonly used model of three-phase relative permeabilities, reasonable values of fluid viscosities are sufficient to preserve strict hyperbolicity.

It also turns out that in three-phase immiscible, incompressible flow with negligible capillarity and gravity, the complete solution of the Riemann problem involves a sequence of two waves, and each wave may only be a rarefaction, a shock, or a rarefaction-shock. Thus there can only be 9 possible combinations of the admissible waves. All these combinations are discussed in our paper. Moreover, the widely used model of three-phase displacement as two successive two-phase displacements is identified as an *approximation* to the full solution. Such approximation is sufficiently accurate only under very restrictive conditions.

The results of this paper will be useful in (a) planning and interpretation of three-phase displacement experiments; (b) obtaining significantly more information from the existing displacement experiments; (c) designing the first complete analytical forward simulator to interpret three-phase displacement experiments; (d) formulating better relative permeability models; and (e) formulating better streamtube simulators of three phase flow.

We will extend the work in this paper as follows: (a) introduce gravity and capillarity; (b) obtain a complete analytical forward model of three-phase flow; (c) develop a new, consistent model of three-phase relative permeabilities; and (d) validate it with experimental data.

Nomenclature

Roman letters

$\boldsymbol{A}$	Jacobian matrix of the system, dimensionless
f	water fractional flow, dimensionless
f_α	fractional flow of the α-phase, dimensionless
$\boldsymbol{f}$	fractional flow vector $[f, g] = [f_w, f_g]$, dimensionless
F_α	mass flux of the α-phase, m/L^{2}t
g	gas fractional flow, dimensionless
g	gravitational acceleration, m/t^2
$\mathcal{H}_p$	Hugoniot locus of the p-characteristic family
$\mathcal{I}_p$	integral curve of the p-characteristic family
$\boldsymbol{I}$	2×2 identity matrix, dimensionless
k	absolute permeability, L^2
$k_{r\alpha}$	relative permeability of the α-phase, dimensionless
m_α	mass of the α-phase p.u. bulk volume, m/L^3
p	global pressure, m/Lt^2
p_α	pressure of the α-phase, m/Lt^2
$\boldsymbol{r}_p$	eigenvector of the p-family, dimensionless
$\mathcal{R}_p$	rarefaction curve of the p-characteristic family
S_α	saturation of the α-phase, dimensionless
$S_{\alpha i}$	immobile saturation of the α-phase, dimensionless
$\tilde{S}_\alpha$	reduced saturation of the α-phase, dimensionless
$\mathcal{S}_p$	shock curve of the p-characteristic family
t	time, t
$\mathcal{T}$	saturation triangle
u	water saturation S_w, dimensionless
$\boldsymbol{u}$	vector of saturations $[u, v] = [S_w, S_g]$, dimensionless
$\tilde{\boldsymbol{u}}$	vector of reduced saturations, dimensionless
$\boldsymbol{U}$	self-similar solution $[u, v]$, dimensionless
v	gas saturation S_g, dimensionless
v_T	total velocity, L/t
$\tilde{v}_T$	reduced total velocity, L/t
v_α	velocity of the α-phase, L/t
$\mathcal{V}_p$	inflection locus of the p-characteristic family
$\mathcal{W}_p$	wave of the p-characteristic family
x	space coordinate, L
z	vertical coordinate, L

Greek letters

δ	discriminant of the eigenvalue problem, dimensionless
ζ	self-similarity variable, dimensionless
λ_T	total mobility, Lt/m
λ_α	relative mobility of the α-phase, Lt/m
μ_α	dynamic viscosity of the α-phase, m/Lt
ν_p	eigenvalue of the p-family, dimensionless
ρ_α	density of the α-phase, m/L^3
σ_p	speed of a shock of the p-characteristic family
ϕ	porosity, dimensionless

Subscripts

$,u$	partial derivative w.r.t. u
$+$	state to the right of a discontinuity
$-$	state to the left of a discontinuity
$*$	post-shock state
1	1-characteristic family
2	2-characteristic family
g	gas phase
l	left state
m	intermediate constant state
o	oil phase
r	right state
w	water phase

Acknowledgements

This work was supported in part by the U.S. Department of Energy under Contract No. DE-AC03-76SF00098. Funding provided by the Jane Lewis fellowship and the Repsol-YPF fellowship, awarded to the first author, is gratefully acknowledged.

References

[1] D. A. DiCarlo, A. Sahni, and M. J. Blunt. The effect of wettability on three-phase relative permeability. *Transp. Porous Media*, 39:347–366, 2000.

[2] G. Chavent and J. Jaffré. *Mathematical Models and Finite Elements for Reservoir Simulation*, volume 17 of *Studies in Mathematics and its Applications*. Elsevier, North-Holland, 1986.

[3] C. Truesdell. *An Idiot's Fugitive Essays on Science — Methods, Criticism, Training, Circumstances*. Springer-Verlag, New York, 1984.

[4] K. Aziz and A. Settari. *Petroleum Reservoir Simulation*. Elsevier, London, 1979.

[5] D. W. Peaceman. *Fundamentals of Numerical Reservoir Simulation*, volume 6 of *Developments in Petroleum Science*. Elsevier, Amsterdam, 1977.

[6] M. Muskat. *Physical Principles of Oil Production*. McGraw-Hill, New York, 1949.

[7] S. K. Godunov. A difference scheme for numerical computation of discontinuous solutions of equations of fluid dynamics (in Russian). *Mat. Sb.*, 47(89):271–306, 1959.

[8] R. J. LeVeque. *Numerical Methods for Conservation Laws*. Birkhäuser Verlag, Berlin, second edition, 1992.

[9] H. J. Welge. A simplified method for computing oil recovery by gas or water drive. *Petrol. Trans.* AIME, 195:91–98, 1952.

[10] G. A. Pope. The application of fractional flow theory to enhanced oil recovery. *SPEJ*, 20(3):191–205, June 1980. *Petrol. Trans.* AIME, 269.

[11] F. G. Helfferich. Theory of multicomponent, multiphase displacement in porous media. *SPEJ*, 21(1):51–62, February 1981. *Petrol. Trans.* AIME, 271.

[12] G. I. Barenblatt. *Scaling, Self-Similarity, and Intermediate Asymptotics*. Cambridge Texts in Applied Mathematics. Cambridge University Press, 1996.

[13] R. D. Wyckoff and H. G. Botset. The flow of gas-liquid mixtures through unconsolidated sands. *Physics*, 7:325–345, 1936.

[14] M. Muskat, R. D. Wyckoff, H. G. Botset, and M. W. Meres. Flow of gas-liquid mixtures through sands. *Petrol. Trans.* AIME, 123:69–96, 1937.

[15] H. G. Botset. Flow of gas-liquid mixtures through consolidated sands. *Petrol. Trans.* AIME, 136:91–105, 1940.

[16] M. C. Leverett and W. B. Lewis. Steady flow of gas-oil-water mixtures through unconsolidated sands. *Petrol. Trans.* AIME, 142:107–116, 1941.

[17] T. M. Geffens, W. W. Owens, D. R. Parrish, and R. A. Morse. Experimental investigation of factors affecting laboratory relative permeability measurements. *Petrol. Trans.* AIME, 192:99–110, 1951.

[18] C. S. Land. Calculation of imbibition relative permeability for two- and three-phase flow from rock properties. *SPEJ*, 8(2):149–156, June 1968. *Petrol. Trans.* AIME, 243.

[19] F. J. Fayers and J. D. Matthews. Evaluation of normalized Stone's methods for estimating three-phase relative permeabilities. *SPEJ*, 24(2):224–232, April 1984. *Petrol. Trans.* AIME, 277.

[20] F. J. Fayers. Extension of Stone's method I and conditions for real characteristics in three-phase flow. In *SPE 62nd Annual Technical Conference and Exhibition*, Dallas, TX, September 27–30, 1987. (SPE 16965).

[21] P. D. Lax. Hyperbolic systems of conservation laws, II. *Comm. Pure Appl. Math.*, 10:537–566, 1957.

[22] T.-P. Liu. The Riemann problem for general 2×2 conservation laws. *Trans. Amer. Math. Soc.*, 199:89–112, 1974.

[23] T.-P. Liu. The Riemann problem for general systems of conservation laws. *J. Differential Equations*, 18:218–234, 1975.

[24] J. B. Bell, J. A. Trangenstein, and G. R. Shubin. Conservation laws of mixed type describing three-phase flow in porous media. *SIAM J. Appl. Math.*, 46(6):1000–1017, 1986.

[25] M. Shearer. Loss of strict hyperbolicity of the Buckley-Leverett equations for three phase flow in a porous medium. In M. F. Wheeler, editor, *Numerical Simulation in Oil Recovery*, volume 11 of *The IMA Volumes in Mathematics and its Applications*, pages 263–283. Springer-Verlag, New York, 1988.

[26] M. Shearer and J. A. Trangenstein. Loss or real characteristics for models of three-phase flow in a porous medium. *Transp. Porous Media*, 4:499–525, 1989.

[27] L. Holden. On the strict hyperbolicity of the Buckley-Leverett equations for three-phase flow. In B. L. Keyfitz and M. Shearer, editors, *Nonlinear Evolution Equations that Change Type*, volume 27 of *The IMA Volumes in Mathematics and its Applications*, pages 79–84. Springer-Verlag, New York, 1990.

[28] L. Holden. On the strict hyperbolicity of the Buckley-Leverett equations for three-phase flow in a porous medium. *SIAM J. Appl. Math.*, 50(3):667–682, 1990.

[29] P. J. Hicks Jr. and A. S. Grader. Simulation of three-phase displacement experiments. *Transp. Porous Media*, 24:221–245, 1996.

[30] D. G. Schaeffer and M. Shearer. The classification of 2×2 systems of nonstrictly hyperbolic conservation laws, with application to oil recovery. *Comm. Pure Appl. Math.*, 40(1):141–178, 1987. Appendix by D. Marchesin and P. J. Paes-Leme.

[31] D. Marchesin and H. B. Medeiros. A note on the stability of eigenvalue degeneracy in nonlinear conservation laws of multiphase flow. In W. B. Lindquist, editor, *Current Progress in Hyperbolic Systems: Riemann Problems and Computations*, volume 100 of *Contemporary Mathematics*, pages 215–224. American Mathematical Society, Providence, RI, 1989.

[32] J. A. Trangenstein. Three-phase flow with gravity. In W. B. Lindquist, editor, *Current Progress in Hyperbolic Systems: Riemann Problems and Computations*, volume 100 of *Contemporary Mathematics*, pages 147–159. American Mathematical Society, Providence, RI, 1989.

[33] R. E. Guzmán. *Mathematics of Three-Phase Flow*. PhD Dissertation, Stanford University, July 1995.

[34] D. Marchesin and B. J. Plohr. Wave structure in WAG recovery. *SPEJ*, 6(2):209–219, June 2001.

[35] E. Isaacson, D. Marchesin, and B. Plohr. Transitional shock waves. In W. B. Lindquist, editor, *Current Progress in Hyperbolic Systems: Riemann Problems and Computations*, volume 100 of *Contemporary Mathematics*, pages 125–145. American Mathematical Society, Providence, RI, 1989.

[36] E. Isaacson, D. Marchesin, B. Plohr, and J. B. Temple. Multiphase flow models with singular Riemann problems. *Mat. Aplic. Comp.*, 11(2):147–166, 1992.

[37] A. H. Falls and W. M. Schulte. Theory of three component, three phase displacement in porous media. *SPERE*, 7(3):377–384, August 1992.

[38] A. H. Falls and W. M. Schulte. Features of three component, three phase displacement in porous media. *SPERE*, 7(4):426–432, November 1992.

[39] M. J. Oak, L. E. Baker, and D. C. Thomas. Three-phase relative permeability of Berea sandstone. *JPT*, 42(8):1054–1061, August 1990.

[40] M. I. van Dijke, K. S. Sorbie, M. Sohrabi, D. H. Tehrani, and A. Danesh. Three-phase flow in WAG processes in mixed-wet porous media: pore-scale network simulations and comparison with micromodel experiments. In *SPE/DOE Thirteenth Symposium on Improved Oil Recovery*, Tulsa, OK, 2002. (SPE 75192).

[41] A. Sahni, R. Guzman, and M. Blunt. Theoretical analysis of three phase flow experiments in porous media. In *SPE 71st Annual Technical Conference and Exhibition*, Denver, CO, October 6–9, 1996. (SPE 36664).

[42] G. Chavent, J. Jaffré, and S. Jan-Jégou. Estimation of relative permeabilities in three-phase flow in porous media. *Inverse Problems*, 15:33–39, 1999.

[43] C. T. Miller, G. Christakos, P. T. Imhoff, J. F. McBride, J. A. Pedit, and J. A. Trangenstein. Multiphase flow and transport modeling in heterogeneous porous media: challenges and approaches. *Adv. Water Resour.*, 21(2):77–120, 1998.

[44] R. Juanes and T. W. Patzek. Relative permeabilities for strictly hyperbolic models of three-phase flow. *Transp. Porous Media*, 2002. (Submitted).

[45] J. S. Osoba, J. G. Richardson, J. K. Kerver, J. A. Hafford, and P. M. Blair. Laboratory measurements of relative permeability. *Petrol. Trans.* AIME, 192:47–56, 1951.

[46] J. G. Richardson, J. K. Kerver, J. A. Hafford, and J. S. Osoba. Laboratory determination of relative permeability. *Petrol. Trans.* AIME, 195:187–196, 1952.

[47] F. N. Schneider and W. W. Owens. Sandstone and carbonate two- and three-phase relative permeability characteristics. *SPEJ*, 10(1):75–84, March 1970. *Petrol. Trans.* AIME, 249.

[48] D. N. Saraf, J. P. Batycky, C. H. Jackson, and D. B. Fisher. An experimental investigation of three-phase flow of water-oil-gas mixtures through water-wet sandstones. In *SPE California Regional Meeting*, San Francisco, CA, March 24–26, 1982. (SPE 10761).

[49] M. J. Oak. Three-phase relative permeability of water-wet Berea. In *SPE/DOE Seventh Symposium on Enhanced Oil Recovery*, Tulsa, OK, April 22–25, 1990. (SPE/DOE 20183).

[50] M. J. Oak. Three-phase relative permeability of intermediate-wet Berea sandstone. In *SPE Annual Technical Conference and Exhibition*, Dallas, TX, October 6–9, 1991. (SPE 22599).

[51] T. W. Patzek. Verification of a complete pore network simulator of drainage and imbibition. *SPEJ*, 6(2):144–156, June 2001.

[52] A. Al-Futaisi and T. W. Patzek. Impact of wettability on two-phase flow characteristics of sedimentary rock: Quasi-static model. *Water Resour. Res.*, 2002. (Submitted).

[53] H. L. Stone. Probability model for estimating three-phase relative permeability. *JPT*, 23(2):214–218, February 1970. *Petrol. Trans.* AIME, 249.

[54] H. L. Stone. Estimation of three-phase relative permeability and residual oil data. *J. Can. Petrol. Technol.*, 12(4):53–61, 1973.

[55] C. M. Dafermos. *Hyperbolic Conservation Laws in Continuum Physics*, volume 325 of *A Series of Comprehensive Studies in Mathematics*. Springer-Verlag, Berlin, 2000.

[56] J. Smoller. *Shock Waves and Reaction-Diffusion Equations*, volume 258 of *A Series of Comprehensive Studies in Mathematics*. Springer-Verlag, New York, second edition, 1994.

[57] F. Ancona and A. Marson. A note on the Riemann problem for general $n \times n$ conservation laws. *J. Math. Anal. Appl.*, 260:279–293, 2001.

[58] R. Juanes and T. W. Patzek. Analytical solution to the Riemann problem of three-phase flow in porous media. *Transp. Porous Media*, 2002. (Submitted).

[59] J. R. Kyte, R. J. Stanclift Jr., S. C. Stephan Jr., and L. A. Rapoport. Mechanism of water flooding in the presence of free gas. *Petrol. Trans.* AIME, 207:215–221, 1956.

[60] G. P. Willhite. *Waterflooding*, volume 3 of *SPE Textbook Series*. Society of Petroleum Engineers, Richardson, TX, 1986.